Phosphorylation promotes activation-induced cytidine deaminase activity at the Myc oncogene

Yunxiang Mu, Monika A. Zelazowska, and Kevin M. McBride

Department of Epigenetics and Molecular Carcinogenesis, The University of Texas MD Anderson Cancer Center, Smithville, TX

Activation-induced cytidine deaminase (AID) is a mutator enzyme that targets immunoglobulin (Ig) genes to initiate antibody somatic hypermutation (SHM) and class switch recombination (CSR). Off-target AID association also occurs, which causes oncogenic mutations and chromosome rearrangements. However, AID occupancy does not directly correlate with DNA damage, suggesting that factors beyond AID association contribute to mutation targeting. CSR and SHM are regulated by phosphorylation on AID serine38 (pS38), but the role of pS38 in off-target activity has not been evaluated. We determined that lithium, a clinically used therapeutic, induced high AID pS38 levels. Using lithium and an AID-S38 phospho mutant, we compared the role of pS38 in AID activity at the Ig switch region and off-target Myc gene. We found that deficient pS38 abated AID chromatin association and CSR but not mutation at Myc. Enhanced pS38 elevated Myc translocation and mutation frequency but not CSR or Ig switch region mutation. Thus, AID activity can be differentially targeted by phosphorylation to induce oncogenic lesions.

The Journal of Experimental Medicine

INTRODUCTION

Activation-induced cytidine deaminase (AID) initiates antibody diversification by introducing U:G mismatches in the Ig genes of activated B lymphocytes. During somatic hypermutation (SHM), AID targets the variable regions of both the Ig heavy and light chain genes, inducing high point mutation rates (10^{-2} to 10^{-3} mutations/bp per generation; Di Noia and Neuberger, 2007). In class switch recombination (CSR), AID targets the noncoding switch regions upstream of constant region exons, inducing double-strand break (DSB) substrates for CSR. Subsequent error-prone processing of uracil by uracil-DNA glycosylase (UNG) base excision repair pathway or, alternatively, mismatch repair MSH2/6 pathways complete SHM and CSR (Stavnezer et al., 2008; Methot and Di Noia, 2017).

The mechanisms that target AID are not Ig exclusive, and AID has widespread off-target association with actively transcribed regions throughout the genome (Chandra et al., 2015; Casellas et al., 2016). AID-dependent mutagenesis and chromosome rearrangement occur at off-target loci, which include oncogenes that are recurrent translocation partners in B cell tumors (Alt et al., 2013; Robbiani and Nussenzweig, 2013). One such example, the oncogenic *Myc/Igh* translocation, is potentiated by AID-initiated DSB at both *Myc* and *Igh* genes (Ramiro et al., 2004; Robbiani et al., 2008). However, even with promiscuous AID association, off-target mutation rates are low compared with *Ig* genes, demonstrating a differential between occupancy and mutation (Liu et al., 2008). AID chromatin binding does not directly correspond to DNA damage (Yamane et al., 2011; Hakim et al., 2012; Matthews et al., 2014), suggesting that factors beyond AID recruitment influence the targeting of AID mutator activity.

AID activity is modulated in vivo by phosphorylation on several residues including serine 3, serine 38, and threonine 140 (McBride et al., 2008; Gazumyan et al., 2011; Le and Maizels, 2015). The best-characterized modification is phosphorylation on AID serine 38 (pS38; Basu et al., 2005). Only a small percentage of total cellular AID is pS38 modified, but it is enriched on chromatin-associated AID (McBride et al., 2006). The role of pS38 in CSR and SHM has been defined with AID serine 38 mutated to alanine (AID^{S38A}) knock-in mice. B cells from these mice support CSR and SHM at 20% of the level of WT mice, demonstrating that pS38 regulates AID activity at the Ig variable and switch regions (McBride et al., 2008; Cheng et al., 2009). However, off-target AID activity has not been evaluated in these mice.

S38 is a consensus site for several kinases (McBride et al., 2008), including the cAMP-dependent protein kinase, PKA (Basu et al., 2005). PKA associates through its regulatory subunit at the Ig switch regions, potentiating AID phosphorylation and activity there. Consistent with this, PKA inhibitors or hypomorphic PKA mutants impair CSR (Pasqualucci et al., 2006; Vuong et al., 2009). DNA damage and activation of ataxia telangiectasia mutated (ATM) facilitate a pS38 positive feedback loop to facilitate CSR (Vuong et al., 2013). Although the switch regions provide an environment rich in DSBs and

Correspondence to Kevin M. McBride: kmcbride@mdanderson.org

Abbreviations used: AID, activation-induced cytidine deaminase; CHX, cycloheximide; CSR, class switch recombination; DSB, double-strand break; IC_{50}, half-maximal inhibitory concentration; SHM, somatic hypermutation; Smu, switch μ; UNG, uracil DNA glycosylase.

The Rockefeller University Press
J. Exp. Med. 2017 Vol. 214 No. 12 3543–3552
https://doi.org/10.1084/jem.20170468

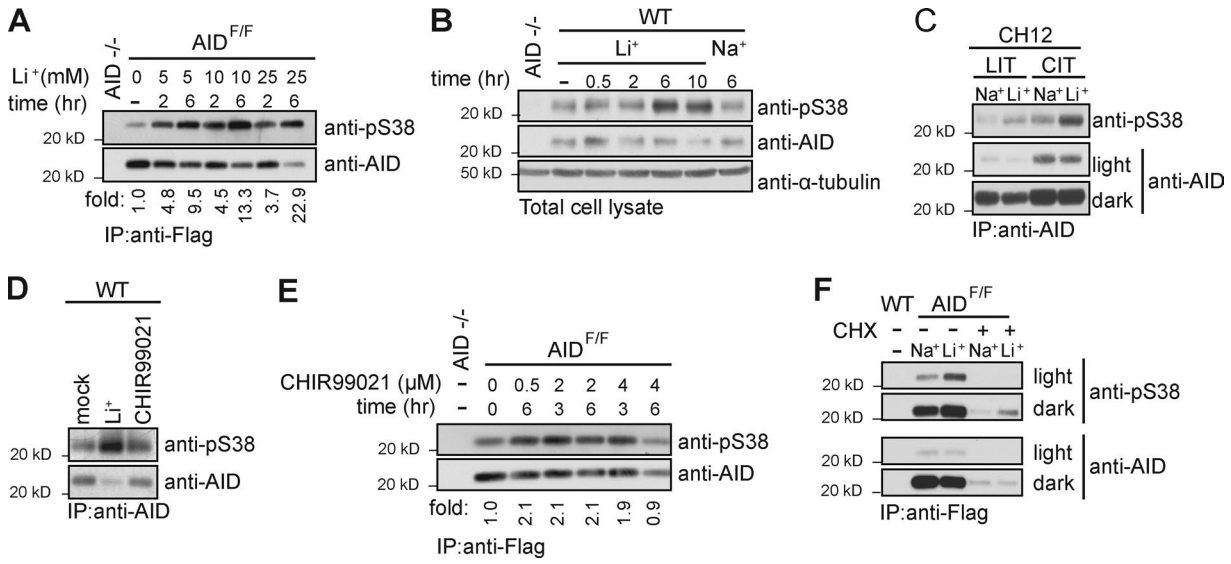

Figure 1. **Lithium treatment induces AID Serine 38 phosphorylation.** (A) Anti-pS38 and anti-AID immunoblot of Flag-AID purified with anti-Flag antibody from lysates of 3-d LPS- and IL-4–stimulated $AID^{F/F}$ B cells treated with indicated concentration of lithium acetate (Li^+) for indicated time before harvest. (B) Anti-pS38, anti-AID, and anti–α-tubulin immunoblot of cell lysates from WT B cells treated with 10 mM LiCl (Li^+) or NaCl (Na^+) as a control for the indicated time. (C) Anti-pS38 and anti-AID immunoblot (light and dark exposures) of AID immunoprecipitated from lysates of CH12 cells cultured with LPS (LIT) or CD40 (CIT) together with IL-4, and TGF-β and treated with 10 mM LiCl or NaCl for 6 h. (D) Representative anti-pS38 and anti-AID immunoblot of AID purified with anti-AID antibody from lysates of WT B cell lysates cultured for 3 d in LPS and IL-4. Cells were treated with 2 μM CHIR99021 or 25 mM LiCl (Li^+) for 6 h before harvest. (E) Anti-pS38 and anti-AID immunoblot of Flag-AID purified with anti-FLAG antibody from cultured $AID^{F/F}$ B cell lysates. Concentration and time of CHIR99021 treatment are indicated. (F) Immunoblot of anti-pS38 and anti-AID (light and dark exposures) of Flag-AID purified with anti-Flag antibody from cell lysates. WT or $AID^{F/F}$ cultured B cells were treated with 10 μg/ml cycloheximide (CHX) 1 h before addition of 10 mM LiCl for 6 h. All panels representative of $n = 3$ independent experiments except F, $n = 2$.

ATM activation, a role for ATM and PKA in regulating pS38 at *Ig* variable regions or off-target genes is not clear.

With an incomplete understanding of signaling pathways that affect AID phosphorylation, we sought to identify pharmacological inhibitors that alter AID pS38. In our studies, we discovered that lithium salts significantly increase pS38. Lithium is used clinically to treat bipolar disorder, depression, and associated mental health disorders (Goodwin et al., 2007), but also modulates several inflammatory and immune functions (Chiu et al., 2013; Maddu and Raghavendra, 2015). Lithium is an inhibitor of glycogen synthase kinase 3 (GSK3; Ryves and Harwood, 2001), which was our original rationale for analysis. However, lithium modulates other signaling pathways and transcription factors unrelated to GSK3 (Lenox and Wang, 2003; Chiu et al., 2013). In this study, we use lithium as a tool to investigate the consequence of altered AID pS38 on AID activity. Together with analysis of AID^{S38A} B cells, we defined the role of pS38 in mutation activity at the Ig switch region, the *Myc* oncogene, and genome-wide off-targets.

RESULTS AND DISCUSSION

Lithium treatment induces AID serine 38 phosphorylation

AID is phosphorylated on S38, and this modification regulates AID activity in SHM, CSR, and gene conversion (Chatterji et al., 2007; McBride et al., 2008; Cheng et al., 2009). Anti-pS38 antibodies have been produced and specifically detect pS38 on AID (Fig. S1 A; McBride et al., 2006, 2008). To determine the impact of lithium on AID pS38 levels, we examined AID from splenocytes stimulated to undergo CSR. We initially used B cells from Flag-tag knock-in AID ($AID^{F/F}$) mice that express functional AID at physiological levels (Pavri et al., 2010). B cells were activated with LPS and IL-4 for 3 d before lithium acetate (LiAc) treatment. We found that LiAc increased pS38 in a time- and dose-dependent manner (Fig. 1 A). This effect was lithium specific, as both LiCl and LiAc (Fig. S1 B) increased pS38 levels, whereas NaCl, used as a control, did not (Fig. 1 B). LiCl induced pS38 in activated primary WT B cells (Fig. 1 B) and in the B cell line CH12 (Fig. 1 C). We concluded that lithium induces pS38 beyond physiological levels. Interestingly, the LiCl induced a small but consistent drop in total AID levels (Fig. S1 C).

Lithium is an inhibitor of GSK3 (half-maximal inhibitory concentration [IC_{50}] 2 mM; Ryves and Harwood, 2001), and this action is thought to contribute to its mood-stabilizing effects. (Klein and Melton, 1996; Chiu et al., 2013). To determine whether GSK3 influences pS38 levels, we treated B cells with the specific GSK3 inhibitor CHIR99021 (IC_{50} 10 nM; Ring et al., 2003). Although treatment with LiCl led to a substantial increase in pS38, CHIR99021 treatment did not (Fig. 1 D). The effect of CHIR99021 on pS38 was a modest ∼2-fold increase with varied time and inhibitor concentrations (Fig. 1 E). We concluded that lithium is not regulating

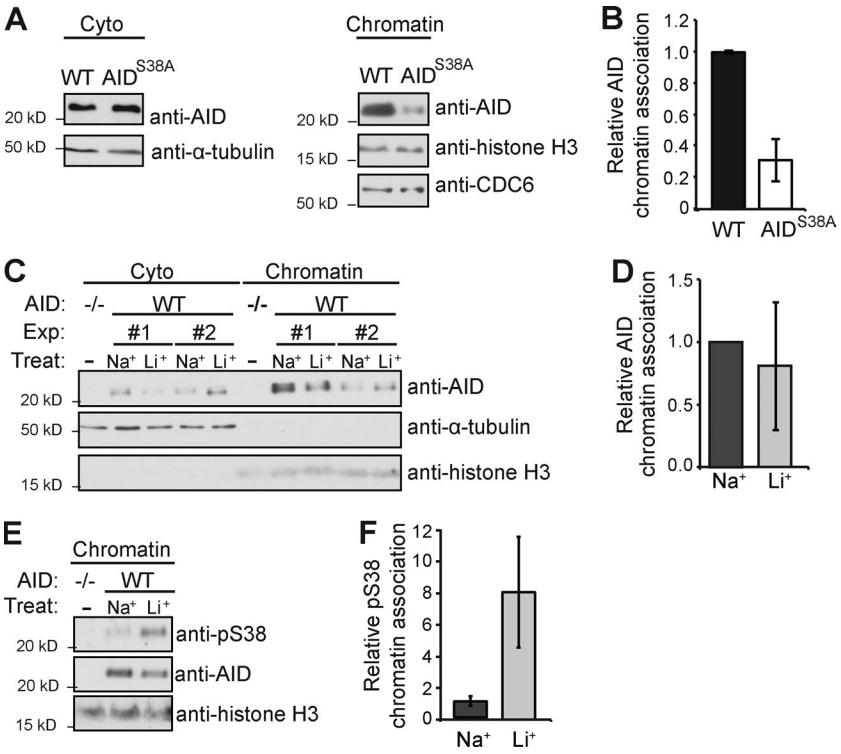

Figure 2. **AID Serine 38 phosphorylation and chromatin association.** (A) Representative anti-AID, anti–α-tubulin, anti–histone H3, and anti-CDC6 immunoblot of the cytoplasmic and chromatin fraction from WT or AID^{S38A} B cells cultured with LPS and IL-4 for 72 h. (B) Summary of relative chromatin levels of $n = 5$ independent experiments. Relative AID signal was normalized to histone H3 level, and WT was arbitrarily set to 1 for each experiment. (C) Representative anti-AID, anti–α-tubulin, and anti–histone H3 immunoblot of the cytosolic and chromatin fraction of LPS- and IL-4–stimulated B cells treated with 10 mM LiCl (Li^+) or NaCl (Na^+) as a control for 12 h. Two independent experiments (Exp) are shown. (D) Summary of relative AID chromatin level from $n = 4$ independent experiments. Relative AID signal was normalized to histone signal, and control (Na^+) was set to an arbitrary value of 1 for each experiment. (B and D) Error bars are SE. (E) Representative anti-pS38, anti-AID, and anti–histone H3 immunoblot of the chromatin fraction from cultured AID$^{-/-}$ or WT B cells treated with 10 mM LiCl or NaCl for 12 h. (F) Summary of mean relative pS38 to AID signal from $n = 3$ independent experiments and SE are displayed.

pS38 through the GSK3 pathway. Lithium has pleiotropic effects in B cells; 12-h LiCl treatment altered phospho-sites on a small subset of proteins regulated by different kinases (Fig. S1 D). Lithium also modulates expression of several genes. To determine whether new protein synthesis is required for LiCl-mediated pS38 induction, we treated B cells with the ribosome translation inhibitor cycloheximide (CHX). 7-h CHX treatment led to a substantial drop in AID levels. However, LiCl treatment resulted in an ∼8-fold increase in pS38 signal regardless of CHX treatment (Fig. 1 F). We concluded that de novo protein synthesis is not required for LiCl to induce pS38.

AID serine 38 phosphorylation and chromatin association

AID must shuttle to the nucleus and associate with chromatin to function. In B cells undergoing CSR, the majority of AID is cytoplasmic, and only a small percentage (5–10%) is associated with chromatin, which is enriched in pS38 (McBride et al., 2006). To determine whether pS38 influences AID chromatin association, we purified the chromatin fraction of B cells from WT or AID^{S38A} mice and determined the relative AID level (Fig. 2, A and B). We found that AID^{S38A} B cells displayed AID chromatin levels ∼30% those of WT cells, suggesting that pS38 promotes chromatin association of AID. To determine whether enhanced pS38 increased AID chromatin association, we analyzed cytosolic and chromatin fractions from LiCl-treated or control NaCl-treated B cells (Fig. 2, C and D). Although LiCl induced no significant change in AID chromatin level, LiCl did significantly increase the pS38 level of AID associated with chromatin (Fig. 2, E and F). These results suggest that a population of nonphosphorylated AID is normally associated with chromatin and that LiCl can enhance pS38 levels on chromatin.

Enhanced AID serine 38 phosphorylation does not increase CSR

AID phosphorylation is required for full activity in CSR. B cells from AID^{S38A} B cells support CSR to IgG1 at ∼20% the rate of WT (McBride et al., 2008; Cheng et al., 2009). To determine whether higher pS38 increases CSR, we analyzed the effect of LiCl on CSR. To distinguish the effect of enhanced pS38 from pleotropic effects of LiCl, we compared CSR to IgG1 in B cells from WT and AID^{S38A} mice (Fig. 3 A). Naive B cells were activated with LPS and IL-4 for 3 d, with 10 mM LiCl or NaCl treatment for the final 12 h before analysis (Fig. 3 A). LiCl-treated WT cells displayed CSR to IgG1 at levels 75% those of controls (Fig. 3, B and C). As expected, AID^{S38A} B cells displayed CSR at rates 20–30% of WT (McBride et al., 2008; Cheng et al., 2009). The addition of LiCl treatment resulted in AID^{S38A} CSR at 80% of NaCl control (Fig. 3, B and C). We found that LiCl treatment of both WT and AID^{S38A} B cells resulted in similar CSR reduction compared with NaCl control. We concluded that increasing pS38 beyond physiological levels does not enhance CSR. The small, but significant, decrease in WT B cell CSR may be caused by pleiotropic effects because we observed a similar, although not significant, trend in AID^{S38A} B cells.

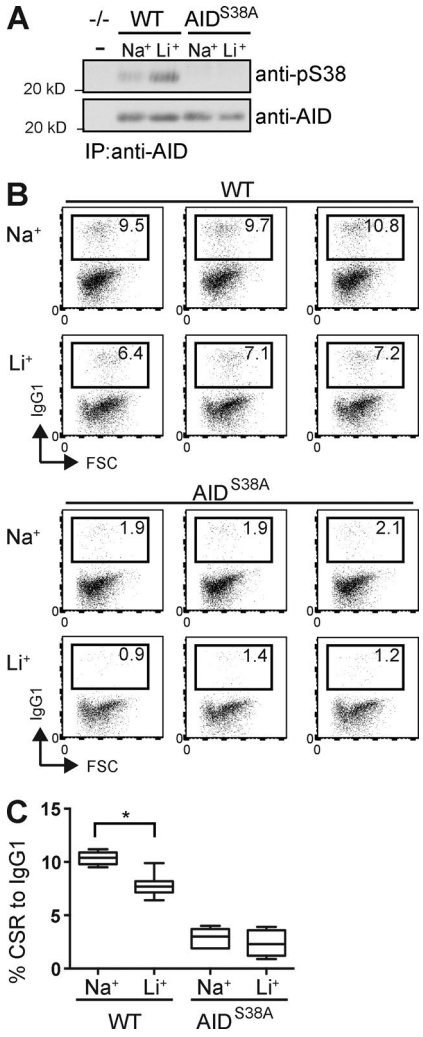

Figure 3. **Enhanced AID Serine 38 phosphorylation does not increase CSR.** (A) Anti-pS38 and anti-AID immunoblot of AID purified with anti-AID antibody from lysates of B cells from WT, AID^{S38A}, or $AID^{-/-}$ mice. Cells were cultured with IL-4 and LPS for 72 h and treated with 10 mM LiCl (Li^+) or NaCl (Na^+) for 12 h before analysis. (B) Representative triplicate FACS plots of CSR to IgG1 in WT and AID^{S38A} B cells from A. Relative percentage of cells expressing IgG1 is in each plot. (C) Summary of CSR to IgG1 in activated B cells from $n = 6$ individual experiments each in triplicate. Error bars are SE. P-value (*, $P < 0.001$) was determined by a two-tailed t test assuming unequal variance.

AID serine 38 phosphorylation promotes *Myc/Igh* translocations

AID activity at off-target sites can induce DSB substrates for chromosome translocations. AID induces the oncogenic *Myc/Igh* translocation by causing DSBs at both *Igh* and *Myc*, with DSBs at *Myc* being rate limiting (Ramiro et al., 2004; Robbiani et al., 2008). The contribution of pS38 to off-target AID activity is not known. Therefore, we determined the effect of increased pS38 on the generation of *Myc/Igh* translocations. We used a previously described PCR/Southern blot assay to determine translocation frequency (Fig. 4 A). LiCl treatment of WT cells resulted in a significant threefold translocation increase compared with control (WT: NaCl control 7, and LiCl 21, translocations from 6.4×10^6 cells; Fig. 4, B and C). AID^{S38A} B cells displayed a translocation frequency similar to that of control WT cells irrespective of LiCl treatment (AID^{S38A}: NaCl control 19, and LiCl 18, translocations from 1.22×10^7 cells; Fig. 4 C). Interestingly AID^{S38A} B cells displayed a lower frequency of amplicons recognized by the *Igh* probe, which sequencing revealed to be internal switch region rearrangements (Fig. 4 A). We conclude that AID generates a background rate of translocations in a pS38-independent manner. However, supraphysiologic pS38 levels induce a significant translocation increase. Because DSBs at *Myc* are a limiting factor in translocation generation, this result is consistent with enhanced pS38 driving DSBs at *Myc*.

Phosphorylation promotes differential targeting of AID mutation activity

To determine whether pS38 regulates AID mutation activity at *Myc*, we analyzed the frequency of AID-induced point mutations. AID associates with *Myc*, but mutation is low because of high-fidelity repair by UNG or mismatch repair (Liu et al., 2008). Indeed, we found that *Myc* mutation frequency in WT B cells was not significantly higher than the PCR error rate regardless of treatment (not depicted). Unrepaired uracils accumulate in the absence of UNG, which results in C:G to T:A transition mutations when replicated. B cells deficient in UNG incur more numerous *Myc* mutations, predominantly at C:G residues (Liu et al., 2008; Yamane et al., 2011). Therefore, we analyzed *Myc* in B cells from $Ung^{-/-}$ mice and focused on mutation at C:G. LiCl induced pS38 to a similar extent in WT and $Ung^{-/-}$ B cells (Fig. 5 A). In $Ung^{-/-}$ cells, LiCl treatment resulted in a fivefold increase in mutation frequency compared with NaCl control, which was near background (Fig. 5 B and Table S1; Liu et al., 2008; McBride et al., 2008). This increase is statistically significant and occurred in the 12-h treatment span. Almost all the LiCl-induced mutations were at C:G sites and were transitions, and most were at AID hotspot (WRC) motifs (Table S1).

To ensure that the LiCl-induced mutations were caused by AID activity, we stimulated $Ung^{-/-}$ B cells with anti-Rp105, which induced proliferation but not AID expression (Fig. 5 C; Callén et al., 2007). In these cells, LiCl did not induce mutation higher than control levels (Fig. 5 B). To demonstrate the role of pS38 in LiCl-induced mutation, we analyzed B cells from $Ung^{-/-}/AID^{S38A}$ double-mutant mice. Myc mutation was not significantly different from background regardless of treatment (Fig. 5 B and Table S1). To boost the sensitivity and directly detect uracils in Myc, we amplified the same genomic DNA with Pfu-Cx, a mutant polymerase that can amplify uracil-containing DNA (Wang et al., 2017). Although we found a mutation frequency higher than background level, there was no difference between LiCl-treated and control NaCl-treated cells (Fig. S2). Strikingly, and in

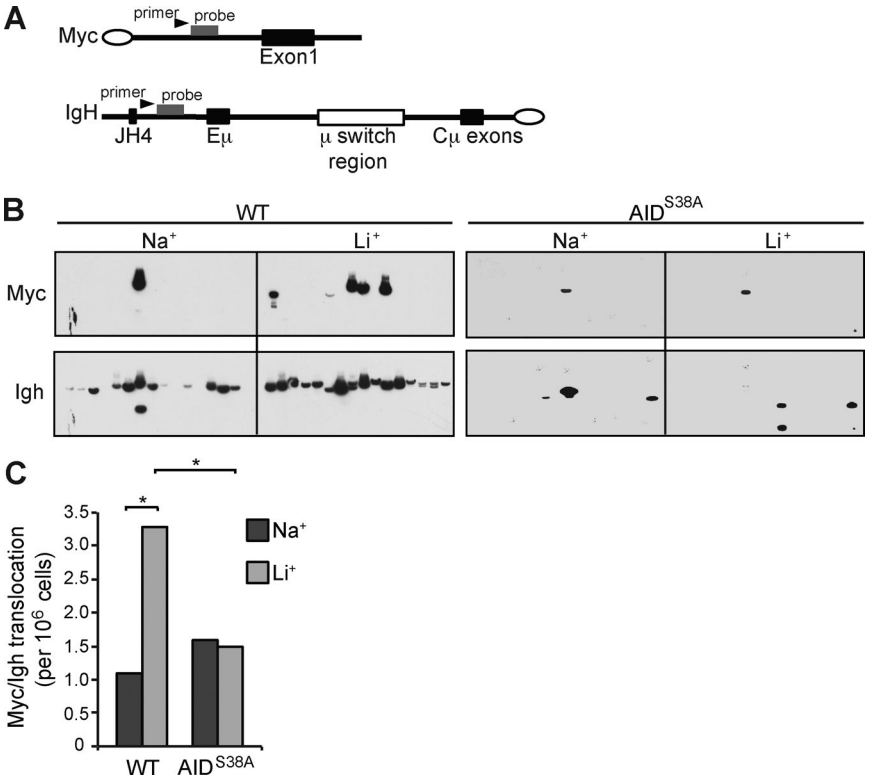

Figure 4. **AID Serine 38 phosphorylation promotes *Myc/Igh* translocations.** (A) Schematic for the *Myc*/*Igh* translocation assay. PCR amplification primers are represented by black arrows and Southern probes by gray bars. Closed circles denote centromeric locations on the chromosomes. (B) Representative translocation assay Southern blots with *Myc* and *Igh* probes are displayed; each lane contains the DNA content of 1×10^5 genomes. B cells from WT or AID^{S38A} mice cultured with IL-4 and LPS were treated with 10 mM NaCl or LiCl for 12 h before analysis. (C) Total translocation frequency summary from $n = 4$ independent experiments. P-values (*, $P < 0.01$) determined using two-tailed Fisher's exact test (WT Na^+ vs. AID^{S38A} Na^+ or Li^+, both $P > 0.5$).

contrast to *Myc*, LiCl treatment resulted in a threefold mutation decrease at the switch μ (Smu) region (Fig. 5 B and Table S1), suggesting dynamic alterations in AID activity targeting.

To ensure that LiCl did not alter target transcription rates, we analyzed the relative levels of Smu region and Myc transcripts (Fig. 5, D and E) by quantitative RT-PCR and observed no change in transcript levels after LiCl treatment. We concluded that LiCl treatment results in differential AID-induced mutation, with an increase at the off-target *Myc* gene and no increase at the on-target Smu region. This is consistent with differential targeting of AID-induced recombination, where an increase in *Myc* translocation coincides with a decrease in CSR (Figs. 3 C and 4 C). Because DSBs at Myc are limiting in the formation of *Myc/Ig* translocations, even the reduced CSR in AID^{S38A} B cells should not be limiting. Our analysis of B cells from AID^{S38A} mice supports the conclusion that pS38 increased AID activity at *Myc*. To determine whether LiCl-induced pS38 increased mutations at other loci, we examined the *Ly6e* and *Il4ra* genes, both reported to be AID targets (Robbiani et al., 2009; Yamane et al., 2011). However, we did not see increased mutation (Table S1), suggesting that not all loci are affected by LiCl-induced pS38. To determine the extent of LiCl-induced AID activity genome-wide, we assessed DSB formation by γH2AX foci formation (Fig. 5 F). Although the percentage of cells with foci was slightly increased in WT LiCl-treated cells (WT: NaCl 68%, LiCl 86%), the number of foci in each γH2AX-positive-staining cell was significantly increased (WT: NaCl 3.8 vs. LiCl 6.7 foci/cell) This increase was AID and pS38 dependent, as it did not occur in $AID^{-/-}$ or AID^{S38A} cells (Fig. 5 G).

Concluding remarks

How AID mutator activity is targeted is a critical question related to lymphomagenesis. AID has promiscuous genomic occupancy, but the involvement of posttranslational modifications in regulating AID off-target activity has not been studied. We show that pS38 is a major contributor to differential mutation activity. AID^{S38A} B cell analysis suggests that pS38 is regulating AID physiological activity at the *Ig* but not the *Myc* locus. Our discovery that LiCl alters AID pS38 levels allowed us to examine the consequences of enhanced pS38 levels. We performed a variety of activity analyses comparing 10 mM LiCl treatment for 12 h (Figs. 2, 3, 4, and 5). Our results suggested that AID phosphorylation can dynamically target AID activity at different genomic locations and contribute to genome instability. Although our γH2AX foci analysis demonstrated that AID activity was increased at multiple loci, mutational analysis of *Il4ra* and *Ly6e* genes suggested that only a subset of AID targets may be affected.

The observed LiCl-induced AID activity might suggest an association of long-term lithium use with lymphoma; however, such a prediction is complicated. Although B cell tumors have been reported in long-term lithium users, significant lymphoma incidence has not. Furthermore, long-term lithium use is actually associated with an overall lower incidence of cancer (Martinsson et al., 2016). Lithium affects several pathways that affect B cell function and are potential

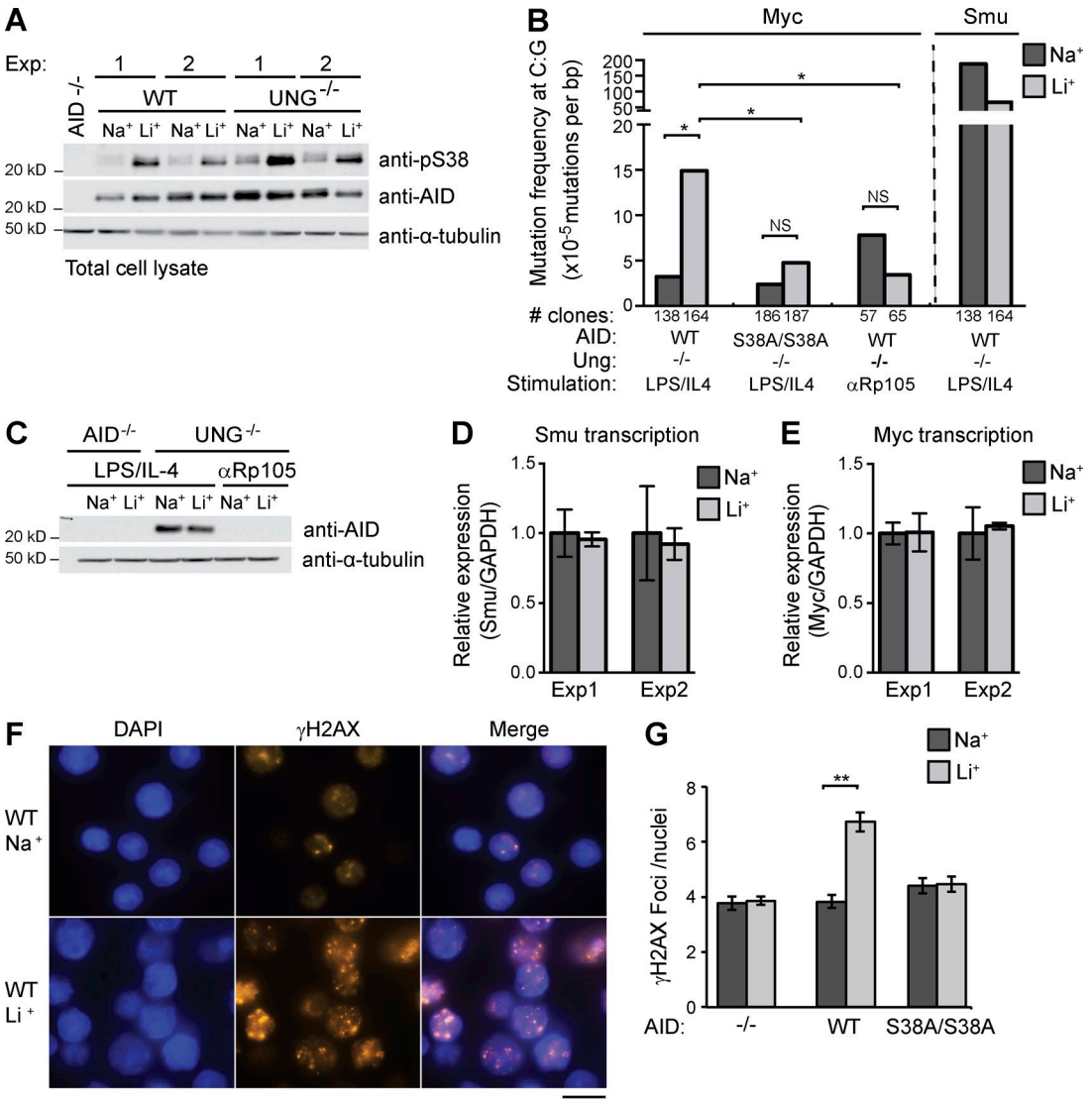

Figure 5. **Phosphorylation promotes differential targeting of AID mutation activity.** (A) Anti-pS38, anti-AID, and anti–α-tubulin immunoblot of cell lysates from AID$^{-/-}$, WT, or Ung$^{-/-}$ B cells activated for 72 h and treated with 10 mM LiCl (Li^+) or control NaCl (Na^+) for 12 h. Two independent experiments displayed. (B) Mutation frequency at C:G bases in *Myc* or *Igh* Smu. B cells from Ung$^{-/-}$ or Ung$^{-/-}$/AID$^{S38A/S38A}$ double-mutant mice were stimulated as indicated. Graph is summary of $n = 5$ independent experiments. Number of clones sequenced indicated. P-values (*, $P < 0.05$) were determined by a two-tailed *t* test assuming unequal variance (*Myc*: WT Na^+ vs. Li^+ and AID^{S38A} Na^+ vs. Li^+, both not significant [NS], $P > 0.4$, Smu: Na^+ vs. Li^+, $P = 0.07$). (C) Anti-AID and anti–α-tubulin immunoblot of lysates from AID$^{-/-}$ or UNG$^{-/-}$ B cells activated with either LPS/IL-4 or anti-Rp105. Representative of $n = 2$ experiments. (D and E) *Igh* Smu germline (D) and *Myc* (E) transcript level analysis. Levels of each transcript from treated B cells were analyzed by quantitative RT-PCR and quantified relative to *Gapdh* transcript levels. Control NaCl sample transcript levels arbitrarily set to 1; $n = 2$ experiments are displayed. Error bars are SE. (F) Representative image of WT B cell nuclei stained with DAPI (blue) and anti-γH2AX (red). Bar, 10 µm. (G) Mean number of foci in nuclei positive for γH2AX staining. Data representative of $n = 3$ experiments (error bars, SEM); **, $P < 0.001$; *t* test.

therapy targets, such as GSK3 in multiple myeloma (Piazza et al., 2013). In this study, we focused on pS38 alterations during short-term LiCl treatment because longer treatment complicates the epigenetic and gene expression landscape. We targeted GSK3 because previous studies suggested that the pathway regulated AID activity in CSR (Omori et al., 2006; Thornton et al., 2016). Although lithium is a GSK3 inhibitor (IC_{50} 2 mM), use of the specific GSK3 inhibitor CHIR99021 did not mimic the effects of lithium. Using CHX, we demonstrated that enhanced pS38 is a direct effect and not caused by gene expression alterations. Quite a number of signaling pathways, including PI3K/Akt, Wnt/B-Catenin, MEK/ERK, oxidative stress, PI/PKC, and cAMP, are affected by lithium (Fig. S1 D; Lenox and Wang, 2003; Chiu et al., 2013). The molecular mechanisms and spectra of pathways modulated by lithium are not completely understood. Altered signaling is a

common feature of lymphomas and a consequence of some therapies, the potential of which to affect genome instability and tumor resistance through AID is only beginning to be realized (Compagno et al., 2017). The unexpected finding that a drug in clinical use can alter AID activity targeting suggests that a more comprehensive picture of the signaling pathways that impact AID phosphorylation is needed.

MATERIALS AND METHODS

Mice

Wild-type, *Aicda*$^{-/-}$ (Muramatsu et al., 2000), *Aicda*$^{F/F}$ (Pavri et al., 2010), *Ung*$^{-/-}$ (Endres et al., 2004), and *Aicda*$^{S38A/S38A}$ (McBride et al., 2008) were on C57BL6/J background. Animals were bred and housed at the accredited University of Texas MD Anderson Cancer Center animal facility. All work was approved by the Institutional Animal Care and Use Committee in accordance with the National Institutes of Health guidelines for use of live animals.

Cell culture and treatment

B cell isolation and culture have been previously described (McBride et al., 2006). Naive B cells were purified from mouse spleens by anti-CD43 bead (Miltenyi Biotec) depletion and cultured in LPS (25 μg/ml; Sigma-Aldrich) and IL-4 (5 ng/ml; Sigma-Aldrich) together or 2.5 μg/ml anti-Rp105/CD180 (BD Biosciences) for 72 h. CH12 cells (Nakamura et al., 1996) were stimulated with TGF-β (1 ng/ml; R&D Systems), IL-4, and either LPS (25 μg/ml) or anti-CD40 antibody (1 μg/ml; eBioscience) for 48 h. Treatments with CHIR 99021 (Selleckchem), cycloheximide (Sigma-Aldrich), NaCl, LiCl, and LiAc (Sigma-Aldrich) were initiated at indicated times before culture harvest and analysis. All NaCl/LiCl treatment comparisons were between cells of the same cultures.

Flow cytometry

For Ig class switch assays, cell suspensions were stained with allophycocyanin-conjugated anti-IgG1 antibodies (BD Biosciences). Samples were acquired on a LSRFortessa (BD) and analyzed with FlowJo (Tree Star). Flow cytometric analysis of surface Ig expression was performed on day 3 of culture with scatter gating and propidium iodide staining to exclude dead cells. Means were obtained from triplicate cultures of six spleens in two independent experiments.

Chromosome translocation assay

The translocation assay has been previously described (Kovalchuk et al., 1997; Ramiro et al., 2004; Gazumyan et al., 2011). Naive B cells were cultured with LPS and IL-4 for 72 h, with LiCl treatment for the final 12 h. PCR reactions (10^5 cells per reaction) were performed with first-round PCR primers, 5′-ACTATGCTATGGACTACTGGGGTCAAG-3′ and 5′-GTGAAAACCGACTGTGGCCCTGGAA-3′, and second-round PCR primers, 5′-CCTCAGTCACCGTCT CCTCAGGTA-3′ and 5′-GTGGAGGTGTATGGGGTG TAGAC-3′, to amplify *Myc*/*Igh* translocations. Amplicons were confirmed as translocations with reactivity to both Southern blot probes *Myc*, 5′-GGACTGCGCAGGGAG ACCTACAGGGG-3′, and *Igh*, 5′-GAGGGAGCCGGC TGAGAGAAGTTGGG-3′. Data are a summary of four independent experiments, and p-values were calculated by two-tailed Fisher's exact test.

Cell lysis and chromatin fractionation

Total cell lysates were made by 30-min RIPA buffer with protease inhibitor (0.2 mM PMSF, 1 μg/ml aprotinin, 1 μg/ml leupeptin, 1 μg/ml pepstatin, and 2 mM EGTA) and phosphatase inhibitor (25 mM NaF, 1 mM sodium orthovanadate, 50 mM disodium β-glycerolphosphate, and 10 mM sodium pyrophosphate) extraction and used for immunoprecipitation or direct Western analysis. Chromatin fractionation was a modification from Perfetti et al. (2015). Cells were lysed in EBC-1 buffer (50 mM Tris-HCl, pH 7.5, 100 mM NaCl, 0.5% NP-40, 1 mM EDTA, 1 mM DTT, 0.2 mM PMSF, 1 μg/ml aprotinin, 1 μg/ml leupeptin, 1 μg/ml pepstatin, 2 mM EGTA, 25 mM NaF, 1 mM sodium orthovanadate, 50 mM disodium β-glycerolphosphate, and 10 mM sodium pyrophosphate). Nuclear pellets were collected, washed in EBC-1, and resuspended in EBC-2 (50 mM Tris-HCl, pH 7.5, 300 mM NaCl, 5 mM $CaCl_2$, 0.2 mM PMSF, 1 μg/ml aprotinin, 1 μg/ml leupeptin, 1 μg/ml pepstatin, 2 mM EGTA, 25 mM NaF, 1 mM sodium orthovanadate, 50 mM disodium β-glycerolphosphate, and 10 mM sodium pyrophosphate) for 30 min. The insoluble chromatin was pelleted, washed with EBC-2, resuspended in RIPA buffer, sonicated, and analyzed as the chromatin-bound fraction.

Antibodies and protein analysis

The antibodies used in this study were anti-pS38 (McBride et al., 2006), anti-AID (30F12 from Cell Signaling Technology or McBride et al. [2004]), and anti–α-tubulin (Sigma-Aldrich). Anti-γH2AX (20E3), anti–histone H3 (D1H2), anti-CDC6 (C42F7), and phospho-substrate antibodies 9611, 2261, and 9621, all from Cell Signaling Technology. Anti-FLAG M2 agarose (Sigma-Aldrich) was used for Flag immunoprecipitation and eluted with Flag peptide. Immunoprecipitated AID or cell lysates (70 μg) were separated on 12% NuPAGE (Invitrogen), transferred to PVDF membrane, probed with anti-pS38 antibody, stripped, and probed with anti-AID and then anti–α-tubulin antibody. Band intensity was quantified with ImageJ, and the ratios of pS38 to AID or AID to H3 signals were calculated. Relative changes were normalized to control samples.

Mutation and DNA damage analysis in primary B cells

Mutations were analyzed in cultured B cells from *Ung*$^{-/-}$ or *Ung*$^{-/-}$*Aicda*$^{S38A/S38A}$ double-mutant mice. B cells were isolated from five separate mice and cultured independently. A fragment from the upstream region of *Igh* Smu region, *Myc*, *Ly6e*, or *Il4ra* genes was amplified with PfuTurbo (Agilent) under the following cycling conditions: 95°C for 3 min, then

25 cycles of 95°C for 30 s, 54°C for Myc and 57°C for Smu for 15 s, 68°C for 2 min, and 72°C for 7 min. Each group was amplified in triplicate and cloned into pCR4-TOPO (Invitrogen), and individual colonies were sequenced. Statistical significance was determined by two-tailed Student's *t* test assuming unequal variance. Primers used (Robbiani et al., 2009;Yamane et al., 2011) were *Sμ*: forward, 5′-GACCCA GGCTAAGAAGGCAATC-3′, and reverse, 5′-GCGGCC CGGCTCATTCCAGTTCATTACAG-3′; *Myc*: forward, 5′-TGGTCTTTCCCTGTGTTCTTTCTG-3′, and reverse, 5′-GACACCTCCCTTCTACACTCTAAACCG-3′; Ly6e: forward, 5′-CTTGGGTGCATTCAGCCTTTG-3′, and reverse, 5′-CCTGAGGAACACCTCCACAAAC-3′; and Il4ra: forward, 5′-GAGCCTGAACTCGCAGGTAG-3′, and reverse, 5′-CCCTCAGTCAGAGAGCACAG-3′.

γH2AX foci formation analysis was performed according to Hasham et al. (2010). Cultured cells were from two mice per experiment. Cells were formaldehyde fixed, permeabilized, blocked, and stained with DAPI, anti–phospho γH2AX antibody, and anti-rabbit secondary antibody. Fluorescence microscopy was preformed with a Zeiss Axiophot, 63× objective, and the mean number of foci per cell was calculated from 150 cells per group.

Quantitative PCR for Myc and germline transcripts

RNA from treated, cultured B cells was extracted with GenElute mammalian total RNA miniprep kit (Sigma-Aldrich), and cDNA was produced with Superscript II reverse transcription (Invitrogen) according to the manufacturer's protocol. Quantitative PCR was performed using Brilliant III SYBR Green Q-PCR Master Mix (Agilent). Reactions were performed in triplicate from B cells of three mice of each genotype. MX3005P Q-PCR software (Stratagene) was used for analysis, and values were normalized to GAPDH. Primers used (Bothmer et al., 2013) were μGLT: forward, 5′-TAGTAAGCGAGGCTCTAA AAAGCA-3′, and reverse, 5′-AGAACAGTCCAGTGT AGGCAGTAGA-3′, and Myc: forward, 5′-TGGAAC TTACAATCTGCGAGCCAG-3′, and reverse, 5′-TCG CTCTGCTGTTGCTGGTGATAG-3′.

Online supplemental material

Fig. S1 shows anti-pS38 antibody recognition of enhanced AID phosphorylation. Fig. S2 shows the mutation frequency of Myc in AID^{S38A} B cells using Pfu-Cx polymerase. Table S1 shows the mutation analysis of *Myc* and *Igh* Smu.

ACKNOWLEDGMENTS

We would like to thank T. Honjo for $Aicda^{-/-}$ mice, R. Jaenisch for $Ung^{-/-}$ mice, and Joshua Plummer for his assistance with flow cytometry and microscopy.

We acknowledge the University of Texas M.D. Anderson Cancer Center (UTMDACC) Research Animal Support Facility (NIH CA16672), flow cytometry core, and molecular biology core. This research was supported by the Welch Foundation (G-1847), Three Strohm Sisters Family Foundation, and UTMDACC Center for Environmental and Molecular Carcinogenesis and Leukemia Specialized Program of Research Excellence (NIH CA100632). Y. Mu was supported by a fellowship from the UTMDACC Center for Cancer Epigenetics.

The authors declare no competing financial interests.

Author contributions: Y. Mu, M. Zelazowska, and K. McBride designed and performed experiments and analyzed data. Y. Mu and K. McBride wrote the manuscript. K. McBride supervised the project.

Submitted: 14 March 2017

Revised: 16 August 2017

Accepted: 26 September 2017

REFERENCES

Alt, F.W., Y. Zhang, F.L. Meng, C. Guo, and B. Schwer. 2013. Mechanisms of programmed DNA lesions and genomic instability in the immune system. *Cell.* 152:417–429. https://doi.org/10.1016/j.cell.2013.01.007

Basu, U., J. Chaudhuri, C. Alpert, S. Dutt, S. Ranganath, G. Li, J.P. Schrum, J.P. Manis, and F.W. Alt. 2005. The AID antibody diversification enzyme is regulated by protein kinase A phosphorylation. *Nature.* 438:508–511. https://doi.org/10.1038/nature04255

Bothmer, A., P.C. Rommel, A. Gazumyan, F. Polato, C.R. Reczek, M.F. Muellenbeck, S. Schaetzlein, W. Edelmann, P.L. Chen, R.M. Brosh Jr., et al. 2013. Mechanism of DNA resection during intrachromosomal recombination and immunoglobulin class switching. *J. Exp. Med.* 210:115–123. https://doi.org/10.1084/jem.20121975

Callén, E., M. Jankovic, S. Difilippantonio, J.A. Daniel, H.T. Chen, A. Celeste, M. Pellegrini, K. McBride, D. Wangsa, A.L. Bredemeyer, et al. 2007. ATM prevents the persistence and propagation of chromosome breaks in lymphocytes. *Cell.* 130:63–75. https://doi.org/10.1016/j.cell.2007.06.016

Casellas, R., U. Basu, W.T. Yewdell, J. Chaudhuri, D.F. Robbiani, and J.M. Di Noia. 2016. Mutations, kataegis and translocations in B cells: understanding AID promiscuous activity. *Nat. Rev. Immunol.* 16:164–176. https://doi.org/10.1038/nri.2016.2

Chandra, V., A. Bortnick, and C. Murre. 2015. AID targeting: Old mysteries and new challenges. *Trends Immunol.* 36:527–535. https://doi.org/10.1016/j.it.2015.07.003

Chatterji, M., S. Unniraman, K.M. McBride, and D.G. Schatz. 2007. Role of activation-induced deaminase protein kinase A phosphorylation sites in Ig gene conversion and somatic hypermutation. *J. Immunol.* 179:5274–5280. https://doi.org/10.4049/jimmunol.179.8.5274

Cheng, H.L., B.Q. Vuong, U. Basu, A. Franklin, B. Schwer, J. Astarita, R.T. Phan, A. Datta, J. Manis, F.W. Alt, and J. Chaudhuri. 2009. Integrity of the AID serine-38 phosphorylation site is critical for class switch recombination and somatic hypermutation in mice. *Proc. Natl. Acad. Sci. USA.* 106:2717–2722. https://doi.org/10.1073/pnas.0812304106

Chiu, C.T., Z. Wang, J.G. Hunsberger, and D.M. Chuang. 2013. Therapeutic potential of mood stabilizers lithium and valproic acid: Beyond bipolar disorder. *Pharmacol. Rev.* 65:105–142. https://doi.org/10.1124/pr.111.005512

Compagno, M., Q. Wang, C. Pighi, T.C. Cheong, F.L. Meng, T. Poggio, L.S. Yeap, E. Karaca, R.B. Blasco, F. Langellotto, et al. 2017. Phosphatidylinositol 3-kinase δ blockade increases genomic instability in B cells. *Nature.* 542:489–493. https://doi.org/10.1038/nature21406

Di Noia, J.M., and M.S. Neuberger. 2007. Molecular mechanisms of antibody somatic hypermutation. *Annu. Rev. Biochem.* 76:1–22. https://doi.org/10.1146/annurev.biochem.76.061705.090740

Endres, M., D. Biniszkiewicz, R.W. Sobol, C. Harms, M. Ahmadi, A. Lipski, J. Katchanov, P. Mergenthaler, U. Dirnagl, S.H. Wilson, et al. 2004. Increased postischemic brain injury in mice deficient in uracil-DNA glycosylase. *J. Clin. Invest.* 113:1711–1721. https://doi.org/10.1172/JCI200420926

Gazumyan, A., K. Timachova, G. Yuen, E. Siden, M. Di Virgilio, E.M. Woo, B.T. Chait, B. Reina San-Martin, M.C. Nussenzweig, and K.M.

McBride. 2011. Amino-terminal phosphorylation of activation-induced cytidine deaminase suppresses c-myc/IgH translocation. *Mol. Cell. Biol.* 31:442–449. https://doi.org/10.1128/MCB.00349-10

Goodwin, F.K., K.R. Jamison, and S.N. Ghaemi. 2007. Manic-Depressive Illness: Bipolar Disorders and Recurrent Depression. Oxford University Press, New York. 1262 pp.

Hakim, O., W. Resch, A. Yamane, I. Klein, K.R. Kieffer-Kwon, M. Jankovic, T. Oliveira, A. Bothmer, T.C. Voss, C. Ansarah-Sobrinho, et al. 2012. DNA damage defines sites of recurrent chromosomal translocations in B lymphocytes. *Nature.* 484:69–74.

Hasham, M.G., N.M. Donghia, E. Coffey, J. Maynard, K.J. Snow, J. Ames, R.Y. Wilpan, Y. He, B.L. King, and K.D. Mills. 2010. Widespread genomic breaks generated by activation-induced cytidine deaminase are prevented by homologous recombination. *Nat. Immunol.* 11:820–826. https://doi.org/10.1038/ni.1909

Klein, P.S., and D.A. Melton. 1996. A molecular mechanism for the effect of lithium on development. *Proc. Natl. Acad. Sci. USA.* 93:8455–8459. https://doi.org/10.1073/pnas.93.16.8455

Kovalchuk, A.L., J.R. Müller, and S. Janz. 1997. Deletional remodeling of c-myc-deregulating chromosomal translocations. *Oncogene.* 15:2369–2377. https://doi.org/10.1038/sj.onc.1201409

Le, Q., and N. Maizels. 2015. Cell cycle regulates nuclear stability of AID and determines the cellular response to AID. *PLoS Genet.* 11:e1005411. https://doi.org/10.1371/journal.pgen.1005411

Lenox, R.H., and L.Wang. 2003. Molecular basis of lithium action: Integration of lithium-responsive signaling and gene expression networks. *Mol. Psychiatry.* 8:135–144. https://doi.org/10.1038/sj.mp.4001306

Liu, M., J.L. Duke, D.J. Richter, C.G.Vinuesa, C.C. Goodnow, S.H. Kleinstein, and D.G. Schatz. 2008. Two levels of protection for the B cell genome during somatic hypermutation. *Nature.* 451:841–845. https://doi.org/10.1038/nature06547

Maddu, N., and P.B. Raghavendra. 2015. Review of lithium effects on immune cells. *Immunopharmacol. Immunotoxicol.* 37:111–125. https://doi.org/10.3109/08923973.2014.998369

Martinsson, L., J. Westman, J. Hällgren, U. Ösby, and L. Backlund. 2016. Lithium treatment and cancer incidence in bipolar disorder. *Bipolar Disord.* 18:33–40. https://doi.org/10.1111/bdi.12361

Matthews, A.J., S. Husain, and J. Chaudhuri. 2014. Binding of AID to DNA does not correlate with mutator activity. *J. Immunol.* 193:252–257. https://doi.org/10.4049/jimmunol.1400433

McBride, K.M., V. Barreto, A.R. Ramiro, P. Stavropoulos, and M.C. Nussenzweig. 2004. Somatic hypermutation is limited by CRM1-dependent nuclear export of activation-induced deaminase. *J. Exp. Med.* 199:1235–1244. https://doi.org/10.1084/jem.20040373

McBride, K.M., A. Gazumyan, E.M. Woo, V.M. Barreto, D.F. Robbiani, B.T. Chait, and M.C. Nussenzweig. 2006. Regulation of hypermutation by activation-induced cytidine deaminase phosphorylation. *Proc. Natl. Acad. Sci. USA.* 103:8798–8803. https://doi.org/10.1073/pnas.0603272103

McBride, K.M., A. Gazumyan, E.M. Woo, T.A. Schwickert, B.T. Chait, and M.C. Nussenzweig. 2008. Regulation of class switch recombination and somatic mutation by AID phosphorylation. *J. Exp. Med.* 205:2585–2594. https://doi.org/10.1084/jem.20081319

Methot, S.P., and J.M. Di Noia. 2017. Molecular mechanisms of somatic hypermutation and class switch recombination. *Adv. Immunol.* 133:37–87. https://doi.org/10.1016/bs.ai.2016.11.002

Muramatsu, M., K. Kinoshita, S. Fagarasan, S.Yamada, Y. Shinkai, and T. Honjo. 2000. Class switch recombination and hypermutation require activation-induced cytidine deaminase (AID), a potential RNA editing enzyme. *Cell.* 102:553–563. https://doi.org/10.1016/S0092-8674(00)00078-7

Nakamura, M., S. Kondo, M. Sugai, M. Nazarea, S. Imamura, and T. Honjo. 1996. High frequency class switching of an IgM+ B lymphoma clone CH12F3 to IgA+ cells. *Int. Immunol.* 8:193–201. https://doi.org/10.1093/intimm/8.2.193

Omori, S.A., M.H. Cato, A. Anzelon-Mills, K.D. Puri, M. Shapiro-Shelef, K. Calame, and R.C. Rickert. 2006. Regulation of class-switch recombination and plasma cell differentiation by phosphatidylinositol 3-kinase signaling. *Immunity.* 25:545–557. https://doi.org/10.1016/j.immuni.2006.08.015

Pasqualucci, L., Y. Kitaura, H. Gu, and R. Dalla-Favera. 2006. PKA-mediated phosphorylation regulates the function of activation-induced deaminase (AID) in B cells. *Proc. Natl. Acad. Sci. USA.* 103:395–400. https://doi.org/10.1073/pnas.0509969103

Pavri, R., A. Gazumyan, M. Jankovic, M. Di Virgilio, I. Klein, C. Ansarah-Sobrinho, W. Resch, A. Yamane, B. Reina San-Martin, V. Barreto, et al. 2010. Activation-induced cytidine deaminase targets DNA at sites of RNA polymerase II stalling by interaction with Spt5. *Cell.* 143:122–133. https://doi.org/10.1016/j.cell.2010.09.017

Perfetti, M.T., B.M. Baughman, B.M. Dickson, Y. Mu, G. Cui, P. Mader, A. Dong, J.L. Norris, S.B. Rothbart, B.D. Strahl, et al. 2015. Identification of a fragment-like small molecule ligand for the methyl-lysine binding protein, 53BP1. *ACS Chem. Biol.* 10:1072–1081. https://doi.org/10.1021/cb500956g

Piazza, F., S. Manni, and G. Semenzato. 2013. Novel players in multiple myeloma pathogenesis: Role of protein kinases CK2 and GSK3. *Leuk. Res.* 37:221–227. https://doi.org/10.1016/j.leukres.2012.10.016

Ramiro, A.R., M. Jankovic, T. Eisenreich, S. Difilippantonio, S. Chen-Kiang, M. Muramatsu, T. Honjo, A. Nussenzweig, and M.C. Nussenzweig. 2004. AID is required for c-myc/IgH chromosome translocations in vivo. *Cell.* 118:431–438. https://doi.org/10.1016/j.cell.2004.08.006

Ring, D.B., K.W. Johnson, E.J. Henriksen, J.M. Nuss, D. Goff, T.R. Kinnick, S.T. Ma, J.W. Reeder, I. Samuels, T. Slabiak, et al. 2003. Selective glycogen synthase kinase 3 inhibitors potentiate insulin activation of glucose transport and utilization in vitro and in vivo. *Diabetes.* 52:588–595. https://doi.org/10.2337/diabetes.52.3.588

Robbiani, D.F., and M.C. Nussenzweig. 2013. Chromosome translocation, B cell lymphoma, and activation-induced cytidine deaminase. *Annu. Rev. Pathol.* 8:79–103. https://doi.org/10.1146/annurev-pathol-020712-164004

Robbiani, D.F., A. Bothmer, E. Callen, B. Reina-San-Martin, Y. Dorsett, S. Difilippantonio, D.J. Bolland, H.T. Chen, A.E. Corcoran, A. Nussenzweig, and M.C. Nussenzweig. 2008. AID is required for the chromosomal breaks in c-myc that lead to c-myc/IgH translocations. *Cell.* 135:1028–1038. https://doi.org/10.1016/j.cell.2008.09.062

Robbiani, D.F., S. Bunting, N. Feldhahn, A. Bothmer, J. Camps, S. Deroubaix, K.M. McBride, I.A. Klein, G. Stone, T.R. Eisenreich, et al. 2009. AID produces DNA double-strand breaks in non-Ig genes and mature B cell lymphomas with reciprocal chromosome translocations. *Mol. Cell.* 36:631–641. https://doi.org/10.1016/j.molcel.2009.11.007

Ryves, W.J., and A.J. Harwood. 2001. Lithium inhibits glycogen synthase kinase-3 by competition for magnesium. *Biochem. Biophys. Res. Commun.* 280:720–725. https://doi.org/10.1006/bbrc.2000.4169

Stavnezer, J., J.E. Guikema, and C.E. Schrader. 2008. Mechanism and regulation of class switch recombination. *Annu. Rev. Immunol.* 26:261–292. https://doi.org/10.1146/annurev.immunol.26.021607.090248

Thornton, T.M., P. Delgado, L. Chen, B. Salas, D. Krementsov, M. Fernandez, S. Vernia, R.J. Davis, R. Heimann, C. Teuscher, et al. 2016. Inactivation of nuclear GSK3β by Ser(389) phosphorylation promotes lymphocyte fitness during DNA double-strand break response. *Nat. Commun.* 7:10553. https://doi.org/10.1038/ncomms10553

Vuong, B.Q., M. Lee, S. Kabir, C. Irimia, S. Macchiarulo, G.S. McKnight, and J. Chaudhuri. 2009. Specific recruitment of protein kinase A to the immunoglobulin locus regulates class-switch recombination. *Nat. Immunol.* 10:420–426. https://doi.org/10.1038/ni.1708

Vuong, B.Q., K. Herrick-Reynolds, B. Vaidyanathan, J.N. Pucella, A.J. Ucher, N.M. Donghia, X. Gu, L. Nicolas, U. Nowak, N. Rahman, et al. 2013. A DNA break- and phosphorylation-dependent positive feedback loop promotes immunoglobulin class-switch recombination. *Nat. Immunol.* 14:1183–1189. https://doi.org/10.1038/ni.2732

Wang, Q., K.R. Kieffer-Kwon, T.Y. Oliveira, C.T. Mayer, K. Yao, J. Pai, Z. Cao, M. Dose, R. Casellas, M. Jankovic, et al. 2017. The cell cycle restricts activation-induced cytidine deaminase activity to early G1. *J. Exp. Med.* 214:49–58. https://doi.org/10.1084/jem.20161649

Yamane, A., W. Resch, N. Kuo, S. Kuchen, Z. Li, H.W. Sun, D.F. Robbiani, K. McBride, M.C. Nussenzweig, and R. Casellas. 2011. Deep-sequencing identification of the genomic targets of the cytidine deaminase AID and its cofactor RPA in B lymphocytes. *Nat. Immunol.* 12:62–69. https://doi.org/10.1038/ni.1964